Environ. Sci. Technol. **2006**, *40,* 215−220

Photodegradation of Decabromodiphenyl Ether Adsorbed onto Clay Minerals, Metal Oxides, and Sediment

MI-YOUN AHN,*,† TIMOTHY R. FILLEY,† CHAD T. JAFVERT,‡ LORING NIES,‡ INEZ HUA,‡ AND JUAN BEZARES-CRUZ‡

Earth and Atmospheric Sciences and School of Civil Engineering, Purdue University, 550 Stadium Mall Drive, West Lafayette, Indiana 47907

The photodebromination of decabromodiphenyl ether (BDE-209) adsorbed onto six different solid matrixes was investigated in sunlight and by irradiation with 350 ± 50 nm lamps (four lamps at 24 W each). After 14 days of lamp irradiation, BDE-209 degraded with a half-life of 36 and 44 days, respectively, on montmorillonite or kaolinite, with much slower degradation occurring when sorbed on organic carbon-rich natural sediment ($t_{1/2}$ = 150 days). In late summer and fall sunlight (40.5°N, elevation 600 ft), the half-lives of BDE-209 sorbed on montmorillonite and kaolinite were 261 and 408 days, respectively. Under both irradiation schemes, no significant loss of BDE-209 occurred when sorbed to aluminum hydroxide, iron oxide (ferrihydrite), or manganese dioxide (birnessite). Upon exposure to both lamp and solar light and in the presence of montmorillonite and kaolinite, numerous lesser brominated congeners (tri- to nonabromodiphenyl ethers) were produced. Nearly identical product distribution was evident on montmorillonite and kaolinite. Dark control experiments for each mineral showed no disappearance of BDE-209 or appearance of degradation products. These results suggest that photodegradation of BDE-209 on mineral aerosols during long-range atmospheric transport may be an important fate process for BDE-209 in the environment.

Introduction

Polybrominated diphenyl ethers (PBDEs) have been produced industrially as flame-retardants since the early 1960s and are found in paints, textiles, and electric and electronic equipment. The market demand for PBDEs (~70 000 metric tons in 2001) has dramatically increased over the years (*1*) with ~86% of the PBDEs distributed to the Americas and Asia (*1*, *2*). Congeners within these commercial mixtures have been detected frequently in sediments, sewage sludge, fish, mammals (including humans), and air throughout the planet (*3*). PBDEs have also been detected in food samples such as cheese and butter (*4*). Their concentration in the environment, as well as foods, appears to have increased over time (*5*). Recently, some PBDEs have been identified as endocrine disruptors, causing neurodevelopmental toxic effects (*6*, *7*).

An intriguing fact is that, although decabromodiphenyl ether (BDE-209) is the major industrial PBDE product, the majority of PBDEs detected in the environment are less brominated congeners (*2*), including tetra and penta congeners found at high concentration in the commercial penta mixture: most notably 2,2′,4,4′-tetrabromodiphenyl ether (BDE-47) and 2,2′,4,4′,5-pentabromodiphenyl ether (BDE-99). Although, these lower molecular weight products were phased out of production in the U.S. and Europe at the end of 2004, the question remains as to whether the congeners typically found in environmental samples originated from these commercial mixtures or from the environmental degradation of BDE-209.

The limited information regarding the fate of BDE-209 in the environment indicates that it may be prone to biotic (*8*) and abiotic (*9*) degradation. Previous studies indicate that photolytic debromination of BDE-209 could be an important abiotic process leading to the formation of less brominated PBDEs. Some studies have shown very facile degradation in organic solvents (*9*, *10*); however, these results are difficult to extrapolate to natural systems due to solvent effects and because most BDE-209 may be sorbed to materials due to its extreme hydrophobicity [log K_{ow} > 8 (*11*)]. Recently, Söderström and co-workers (*12*) studied the photodegradation of BDE 209 sorbed onto silica gel, sand, sediment, and soil, showing that different adsorbents produced various debrominated products (tetra- to nona-BDEs) over time. Hua et al. (*13*) showed that BDE-209 also photodegraded when it was adsorbed to humic acid-coated sand particles with similar appearance of lower molecular weight congeners. However, information about how the major components of soil/sediment/mineral aerosols, such as 2:1/1:1 clay minerals or noncrystalline metal oxides, which are known to have electron transferring capacities, affect the photodegradation of BDE-209 is unknown. Therefore, it is critical to expand the investigation of the photolysis of BDE-209 immobilized on specific soil/sediment/mineral aerosol components. Degradation rates of other organic pollutants sorbed on solids varies depending on the kind of clay minerals (*14*−*17*). When organic compounds are in the sorbed state, their photodegradation is often highly dependent on the chemical and physical properties of the sorbent (*14*, *18*, *19*). The rate of degradation may be accelerated through energy transfer reactions, through light adsorption or efficient light scattering, or it may be reduced via excited-state quenching or by radiation shielding (*14*−*16*). In addition, many sorbents, including some minerals, may act as electron donors during photodegradation (*20*).

Photodegradation of BDE-209 on particles may be an important issue when considering the global environmental distribution of PBDEs. Global transport of PBDEs needs further investigation. The detection of several of the less halogenated congeners in remote regions (*21*) suggests that considerable atmospheric transport occurs, and it is possible that sorption onto airborne particulates accounts for at least part of this transport. Whether carried on particles or carried directly through the gas phase, it is likely that photodegradation plays a role in the fate of BDE-209 in the global environment.

To examine these possible effects in this study, the rate of photochemical transformation of BDE-209 adsorbed onto clay minerals (montmorillonite and kaolinite), metal oxides (manganese dioxide; birnessite, iron oxide; ferrihydrite, and aluminum hydroxide), and natural sediment in water was investigated. Previous reports on the composition of mineral aerosols showed that montmorillonite and kaolinite were

* Corresponding author phone: +765-494-3274; fax: +765-496-1210; e-mail: mahn@purdue.edu.
† Earth and Atmospheric Sciences.
‡ School of Civil Engineering.

10.1021/es051415t CCC: $33.50 © 2006 American Chemical Society
Published on Web 11/23/2005

the major components (*22*, *23*), and these are also the principal clay minerals of the northern hemisphere soils and sediments (up to >700 g kg^{-1}) (*24*). Therefore, our study focused mainly on montmorillonite and kaolinite, which catalyzed the most significant loss of BDE-209 in our experiments. Additionally, we report on the identity of many of the resulting products on both minerals and suggest this work is a significant contribution to understanding the global distribution of PBDEs.

Materials and Methods

Chemicals. Decabromodiphenyl ether (BDE-209; 98% purity) and hexachlorobenzene, used as an internal standard, were obtained from Aldrich Chemical Co. (Milwaukee, WI). A mixture of 39 PBDE congeners (EO-5113) each having from one to seven bromine atoms, was obtained from Cambridge Isotope Lab, Inc, and seven individual congeners (BDE-77, -156, -184, -191, -196, -206, and -207) were purchased Wellington Laboratories (Table 1).

Adsorbents. The solid sorbents were selected to provide a range of characteristics and included clay minerals, metal oxides, and sediment. Panther Creek Na^+-montmorillonite (a 2:1 clay mineral; smectite) and Florida kaolinite (a 1:1 clay mineral) were purchased from Ward's Natural Sciences (Rochester, NY); surface areas are 31 and 33 m^2 g^{-1}, respectively, calculated by a N_2 adsorption technique (*25*). The sediment was collected from the Celery Bog Park, West Lafayette, Indiana, and was characterized by Turf Diagnostics and Design (Linwood, KS) as loam sediment. The sediment (pH 6.3) was oven-dried at 50 °C and passed through a 2-mm sieve prior to use. The organic carbon content was measured with a Carlo Erba 1108 elemental analyzer at 16.4%.

Three metal oxides were synthesized in the laboratory. Iron oxide, ferrihydrite, was synthesized according to the method of Schwertmann and Cornell (*26*). Manganese dioxide, birnessite, was prepared according to the method of McKenzie (*27*). Aluminum hydroxide was synthesized by gradual neutralization of a 0.5 M $AlCl_3$ solution to pH 7 using 0.5 M NaOH (*28*). Analysis of three metal oxides by X-ray diffraction using a PADV X-ray diffractometer with a Co Kα radiation source (Scintag, Inc., Cupertino, CA) and infrared spectroscopy using a Nexus 670 Fourier transform infrared spectrophotometer (Thermo Electro Co., Waltham, MA) showed the presence of poorly crystalline minerals, with characteristic peaks matching those reported in the literature (*26*−*28*). Specific surface areas of birnessite, ferrihydrite, and aluminum hydroxide were 28, 251, and 298 m^2 g^{-1}, respectively. They were determined by N_2 sorptometry on a model ASAP 2021 sorptometer (Micromeretics, Londonberry, NH).

Experimental Setup. BDE-209 stock solution (100 μL) containing 1.0 mg mL^{-1} in tetrahydrofuran (THF) was added to 250 mg of either montmorillonite, kaonilite, a metal oxide, or sediment in 15 mL glass-culture tubes (81 ± 2% of transmittance at 300−400 nm, measured by UV spectrometer), and the THF was removed by air-drying for 30 h in the dark. Each sample in a test tube was homogenized, and 500 μL of water was added to the mixture and sealed with Teflon-lined caps. Sample clumps in the bottom of the test tubes were irradiated either with sunlight or within a photochemical reactor.

The reactor was a Rayonet RPR-100 photochemical chamber reactor (Southern New England Ultraviolet, Branford, CT) equipped with four black light-phosphor UV lamps (24 W). The maximum light intensity of the lamps occurs near 350 nm, with a nearly bell-shaped intensity distribution occurring from approximately 300−400 nm (approximately 1.0 W m^{-2} nm^{-1}). Samples were rotated past the light source at a speed of 5 rpm up to 2 weeks. Samples were collected at 0, 1, 2, 3, 7, and 14 days after initiation of the irradiation. The solar irradiation experiments were performed from July to November 2004, in West Lafayette, IN, with sampling occurring at 0, 14, 28, 56, and 101 days; further exposure in late November/December did not result in further photodegradation of BDE-209. Sample tubes were placed on a wooden board at an angle of 45°. All samples were rotated 120° once every week. A record of the mean temperature (daily average, °C) and intensity of solar radiation (daily average, W m^{-2}) during the experimental period was obtained from the Meteorological Station at the Agricultural Center for Research and Education (86.99W, 40.47N) located at Purdue University within 5 miles of where the samples were exposed (Figure 1). Maximum UV-irradiance (368 nm) from sun at midday was 0.7 W m^{-2} nm^{-1} on July 28, 2004. Dark control samples covered with aluminum foil were prepared and exposed in both the reactor and solar irradiation experiments. At each sampling time, triplicate tubes were removed from light exposure, and BDE-209 and organic products were extracted from the solid phase by vigorously mixing with three sequential 2-mL volumes of THF. The three

TABLE 1. Relative Retention Times of Standards (Retention Order)

Br atoms	BDE no.	IUPAC name	RT GC-ECD (min)[a]
1	BDE-1	2-bromodiphenyl ether	0.68
	BDE-2	3-bromodiphenyl ether	0.70
	BDE-3	4-bromodiphenyl ether	0.73
2	BDE-10	2,6-dibromodiphenyl ether	2.07
	BDE-7	2,4-dibromodiphenyl ether	2.18
	BDE-11	3,3′-dibromodiphenyl ether	2.24
	BDE-8	2,4′-dibromodiphenyl ether	2.24
	BDE-12	3,4-dibromodiphenyl ether	2.27
	BDE-13	3,4′-dibromodiphenyl ether	2.31
	BDE-15	4,4′-dibromodiphenyl ether	2.31
3	BDE-30	2,4,6-tribromodiphenyl ether	2.50
	BDE-32	2,4′,6-tribromodiphenyl ether	2.60
	BDE-17	2,2′,4-tribromodiphenyl ether	2.63
	BDE-25	2,3′,4-tribromodiphenyl ether	2.63
	BDE-33	2′,3,4-tribromodiphenyl ether	2.67
	BDE-28	2,4,4′-tribromodiphenyl ether	2.67
	BDE-35	3,3′,4-tribromodiphenyl ether	2.69
	BDE-37	3,4,4′-tribromodiphenyl ether	2.73
4	BDE-75	2,4,4′,6-tetrabromodiphenyl ether	2.87
	BDE-49	2,2′,4,5′-tetrabromodiphenyl ether	2.89
	BDE-71	2,3′,4′,6-tetrabromodiphenyl ether	2.91
	BDE-47	2,2′,4,4′-tetrabromodiphenyl ether	2.93
	BDE-66	2,3′,4,4′-tetrabromodiphenyl ether	2.97
	BDE-77	3,3′,4,4′-tetrabromodiphenyl ether	3.02
5	BDE-100	2,2′,4,4′,6-pentabromodiphenyl ether	3.11
	BDE-119	2,3′,4,4′,6-pentabromodiphenyl ether	3.12
	BDE-99	2,2′,4,4′,5-pentabromodiphenyl ether	3.15
	BDE-116	2,3,4,5,6-pentabromodiphenyl ether	3.18
	BDE-118	2,3′,4,4′,5-pentabromodiphenyl ether	3.19
	BDE-85	2,2′,3,4,4′-pentabromodiphenyl ether	3.25
	BDE-126	3,3′,4,4′,5-pentabromodiphenyl ether	3.25
6	BDE-155	2,2′,4,4′,6,6′-hexabromodiphenyl ether	3.26
	BDE-154	2,2′,4,4′,5,6′-hexabromodiphenyl ether	3.30
	BDE-153	2,2′,4,4′,5,5′-hexabromodiphenyl ether	3.38
	BDE-138	2,2′,3,4,4′,5′-hexabromodiphenyl ether	3.53
	BDE-166	2,3,4,4′,5,6-hexabromodiphenyl ether	3.55
7	BDE-183	2,2′,3,4,4′,5′,6-heptabromodiphenyl ether	3.73
	BDE-181	2,2′,3,4,4′,5,6-heptabromodiphenyl ether	4.00
	BDE-190	2,3,3′,4,4′,5,6-heptabromodiphenyl ether	4.04
8	BDE-197	2,2′,3,3′,4,4′,6,6′-octabromodiphenyl ether	4.47
	BDE-196	2,2′,3,3′,4,4′,5,6′-octabromodiphenyl ether	4.54
9	BDE-208	2,2′,3,3′,4,5,5′,6,6′-nonabromodiphenyl ether	5.64
	BDE-207	2,2′,3,3′,4,4′,5,6,6′-nonabromodiphenyl ether	5.79
	BDE-206	2,2′,3,3′,4,4′,5,5′,6-nonabromodiphenyl ether	6.14
10	BDE-209	2,2′,3,3′,4,4′,5,5′,6,6′-decabromodiphenyl ether	8.67

[a] RT is relative retention time, normalized to retention time of hexachlorobenzene.

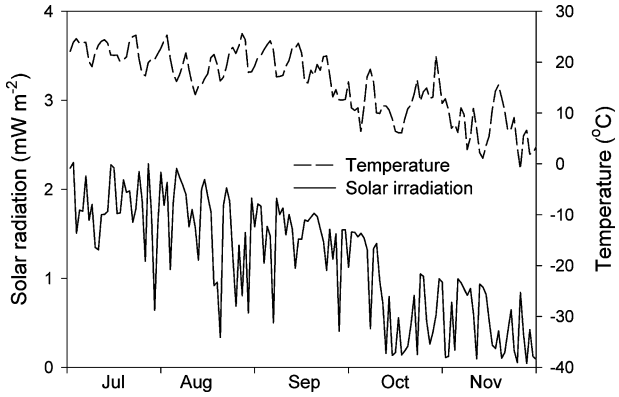

FIGURE 1. Daily average temperature and solar light intensity during the exposure period.

THF volumes were combined and filtered through a 0.2-μm nylon membrane prior to HPLC analysis.

Desorption experiments were completed using a series of THF and water mixtures (v/v, 0:10, 1:9, 2:8, 3:7, 4:6, 5:5, 6:4, and 7:3). BDE-209 (2.5 μg mg^{-1}) in THF was adsorbed on 100 mg of each mineral, and THF was completely removed. Desorption was performed by adding 5 mL of a THF and water mixture and shaking the samples for 24 h at 25 °C. Following centrifugation and filtration through a 0.2-μm nylon membrane, the concentration of BDE-209 in the supernatant was analyzed by HPLC.

HPLC Analysis. BDE-209 in samples was quantified with a Varian 9050 HPLC system monitoring at 240 nm, using the Supelcosil LC-18 DB column (length = 10 cm, i.d. = 4.6 mm, film thickness = 5-μm; Supelco, Bellefonte, PA). The mobile phase was 2% water in acetonitrile delivered isocratically (*13*). The retention time of a peak for BDE-209 was 6.2 min, and the quantification was done with a five-point calibration curve with a BDE-209 standard.

Product Analysis. Prior to GC-ECD analysis, polar compounds including water were removed from each sample by passing them through dried Na_2SO_4, and THF was removed from each resultant sample by a stream of N_2. BDE-209 and products were redissolved in 2 mL of hexane, and an internal standard was added to all samples before the analysis with a Hewlett-Packard (Agilent Technologies) 5890 II gas chromatograph (GC) equipped with an electron capture detector (ECD), a programmable pressure on-column injection port, and a DB5-MS capillary column (length = 30 m, i.d. = 0.25 mm, film thickness = 0.25 μm). The carrier gas was He and the makeup gas was N_2. The initial oven temperature was 100 °C, and it was maintained there for 2 min, increased by 5 °C min^{-1} to 200 °C, and then increased by 10 °C min^{-1} to 285 °C; the temperature was held at 285 °C for 60 min, increased at 10 °C min^{-1} to 330 °C, and held for 5 min. Product identification was based on matching retention times of PBDE standards listed in Table 1 to retention times of product peaks. Unknown congeners were assigned to homologue groups based on relative retention times obtained from the literature (*9*). Quantification for congeners contained in the calibration mixture was done by comparing the relative response factor to the internal standard. Other congeners were quantified by calculating an average homologue group response factor from known congeners.

Results and Discussion

BDE-209 Photodegradation. Foil-covered dark controls for all six solid-phase samples showed no disappearance of BDE-209 during UV and sunlight irradiation. Light controls without minerals exhibited no direct photodegradation of BDE-209. As shown in Table 2, the photodegradation occurred more rapidly with the lamps than with sunlight, due to the higher continuous light intensity in the reactor than in the diurnal solar light. The calculated half-lives of BDE-209 sorbed onto six sorbents are presented in Table 2. Half-lives were determined by assuming a first-order kinetic where [BDE-209] = $[\text{BDE-209}]_0 e^{-kt}$; [BDE-209] is the BDE-209 concentration at a given time, t; $[\text{BDE-209}]_0$ is the initial concentration of BDE-209; and k is the rate constant. After 14 days of irradiation in the reactor, BDE-209 loss on the six sorbents showed reactivity corresponding to the following order: montmorillonite > kaolinite > sediment > aluminum hydroxide > birnessite > ferrihydrite (Table 2).

TABLE 2. Half-Lives ($t_{1/2}$) and Rate Constants (k) of BDE-209 Adsorbed on the Minerals and Sediment with the Assumption of First-Order Reaction

sorbents/ solvents	UV		sunlight	
	$t_{1/2}$	k (d^{-1})	$t_{1/2}$	k (d^{-1})
montmorillonite	36 d	0.0192 ± 0.0067	261 d	0.0032 ± 0.0009
kaolinite	44 d	0.0158 ± 0.0012	408 d	0.0017 ± 0.0003
sediment	150 d	0.0046 ± 0.0003	990 d	0.0007 ± 0.0003
	40−60 h[b]		80 h[b]	
	53 h[c]		81 h[c]	
Al hydroxide	178 d	0.0039 ± 0.0007		—[a]
Mn dioxide (birnessite)	1423 d	0.0005 ± 0.0002		—[a]
Fe oxide (ferrihydrite)		—[a]		—[a]
sand[b−d]	12 h[b]		37 h[b]	
	12 h[c]		37 h[c]	
			533 h[d]	
soil[b,c]	150-200 h[b]			
	185 d[c]			
silica gel[b]	<0.25 h[b]			
toluene[b,c]	<0.25 h[b,c]			
hexane[e]			<0.2 h[e]	0.0011 (s^{-1})[e]
methanol/ water[f]	0.5 h[f]			
methanol	0.85 h[f]			
tetrahydrofuran	1−1.5 h[f]			

[a] $k \approx 0$. [b] Reference *12*. [c] Reference *29*. [d] Reference *13*. [e] Reference *9*. [f] Reference *10*.

There was no significant loss of BDE-209 sorbed on aluminum hydroxide, ferrihydrite, or birnessite after sunlight irradiation for 101 days; however, on montmorillonite, kaolinite, and sediment, degradation occurred with half-lives of 216, 408, and 990 days, respectively (Table 2). Half-life data measured in this study are considerably longer than other published data as Table 2 shows. For example, half-lives of BDE-209 on sediment in other studies (*12*, *29*) were shorter than our results, which are likely due to differences in experimental setup and conditions, such as light intensity and sample size. For example, sample size will affect the fraction of solid surface area that is irradiated. In addition, previously published data showed that BDE-209 adsorbed to more complex matrixes, i.e., sediment or soil, and an organic matter containing matrix has a longer half-life (*12*, *13*, *29*). This is in agreement with our study where sediment has a longer half-life than the more well-defined surfaces of montmorillonite or kaolinite. It clearly indicates that those clay minerals are an important factor for catalyzing photodegradation of BDE-209, while organic matter in the matrix may not stimulate photodegradation.

The different degradation rates could be related to the interaction with clay minerals. BDE-209 is expected to be sorbed to all absorbents by weak physical (van der Waals) and hydrophobic attraction as their bonding forces. Figure 2 shows that montmorillonite has a stronger affinity for BDE-

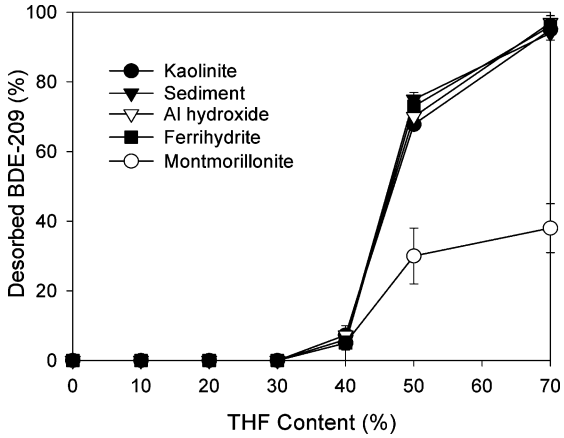

FIGURE 2. Percent of BDE-209 desorbed from minerals by a range of different THF and water mixtures (0:10 to 7:3, v/v) after 24 h at 25 °C. Birnessite mediated a dark reaction with BDE-209 in the presence of THF; therefore, data is not presented.

209 than other minerals; for example, 31 ± 6% of BDE-209 was desorbed from montmorillonite while 69 ± 9% was desorbed from kaolinite and two metal oxides in a THF: water (5:5) mixture. The greater affinity of BDE-209 to montmorillonite over other minerals does not appear to be a function of mineral surface areas (31, 32, 28, 251, and 298 $m^2 g^{-1}$ for montmorillonite, kaolinite, birnessite, ferrihydrite, and aluminum hydroxide, respectively). Since montmorillonite and kaolinite each have significantly different bonding affinities for BDE-209 but degrade it at relatively similar rates, we conclude that bonding forces do not have an effect on the photodegradation rate.

Our results showing that photodegradation of BDE-209 is enhanced by the presence of some clay minerals, such as montmorillonite or kaolinite (Table 2), is consistent with previous studies (*16*), and it has been proven that photolysis rates within the photic zone are greater in turbid than in clear water bodies (*15*). Since reductive debromination requires a source of electrons, this may be the result of the electron-donating ability of the clay minerals during the irradiation process. Smectites, such as montmorillonite, are known to be electron donors during photolysis arising from the bridging Si−O−Al oxygen or crystal edges (*21*). The bridging oxygens in the Si−O−Al clay structure have a high electron density, and the light-excited BDE-209 may obtain electrons from the oxygens. None of the metal oxides (Mn, Fe, and Al oxides) used in this study exhibited any sign of enhancement of the photodegradation of BDE-209 (Table 2). Compared to montmorillonite or kaolinite, metal oxides tend to exist in smaller amounts in environmental samples (*24*); therefore, the results for metal oxides here may not be a significant factor on controlling the photodegradation rate of BDE-209. However, some metal oxides, such as Mn, Zn, Fe, or Ti oxides, are known semiconductors that can act as photocatalysts, and future mechanistic studies of PBDE photodegradation with additional minerals are justified (*14*, *30*, *31*).

In this study, BDE-209 on montmorillonite and kaolinite showed a similar photodegradation rate (Table 2, Figure 3), although the optical properties (light absorption and scattering) for kaolinite and montmorillonite are significantly different. Ciani and Goss (*19*) showed that light absorption was much greater for montmorillonite than kaolinite, but scattering occurred to a greater extent with kaolinite than montmorillonite under irradiation of 300−400 nm. Clearly, light absorption and scattering, together, affect the rate of chemical degradation in complex ways that are difficult to predict quantitatively.

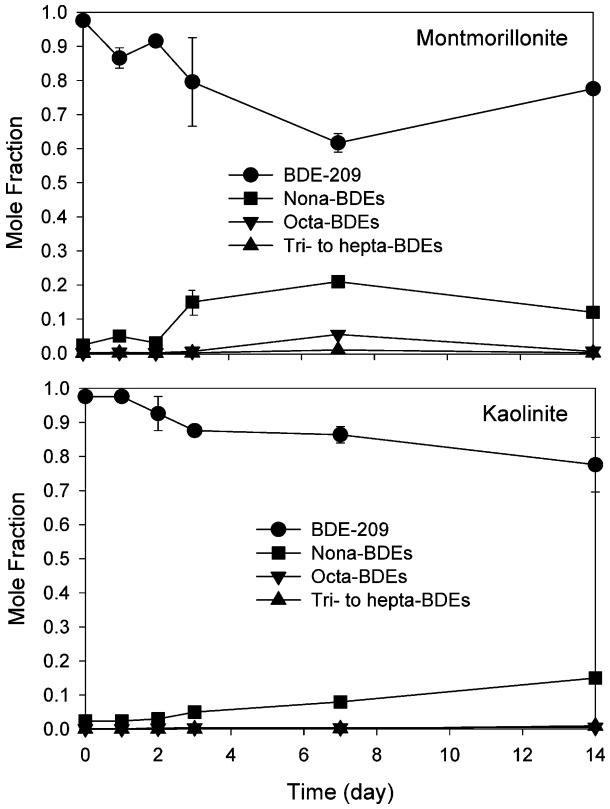

FIGURE 3. Mole fraction distribution of BDE-209 and its products after irradiation in the reactor (300 nm < λ < 400 nm) (n = 3 for each datum point). To calculate the mass balance, all peak areas within the retention time ranges of each structural isomer group were quantified with the average response factor (normalized to response of hexachlorobenzene) of the standard isomers.

There was limited photodegradation of BDE-209 on the sediment compared to kaolinite or montmorillonite (Table 2). Light penetration depth in soils (0.17−0.3 mm) for 275−700 nm is similar or greater to that of pure clay minerals (*19*). Hence, the difference in photodegradation rates between sediment and clay minerals in this study is not likely due to differences in light penetration. Previous reports have found organic matter can either enhance or inhibit the rate of photolysis (*32*). A study by Miller and Zepp (*33*) showed that photodegradation rates of two hydrophobic chemicals in sediments with varied organic matter contents were different. An increased rate of degradation was obtained in sediment with lower organic matter content. The organic matter may inhibit the photodegradation of organic chemicals by either shielding the organic pollutants from available light or by quenching the excited states of the organic molecules before they react to form products (*34*). The inhibitory effect of dissolved organic matter on photodegradation of BDE-209 was studied by Hua et al. (*13*), where BDE-209 in contact with a humic acid solution exhibited a slower photodegradation rate than in the absence of humic acid. They also showed that BDE-209 sorbed to humic acid-coated sand particles photodegraded more slowly than BDE-209 adsorbed to uncoated sand. The limited photodegradation of BDE-209 in natural sediment containing organic matter in this study (Table 2) is consistent with this previous study.

Previously, the photocatalytic role of soil components in the generation of hydroxyl radicals has been studied. Photogeneration of hydroxyl radical might be derived from water on the surfaces of kaolinite or montmorillonite (*17*), and transition metals act as photocatalysts by generating a hydroxyl radicals (*14*, *17*, *35*, *36*). However, there was no significant photodecomposition on the surfaces of ferrihy-

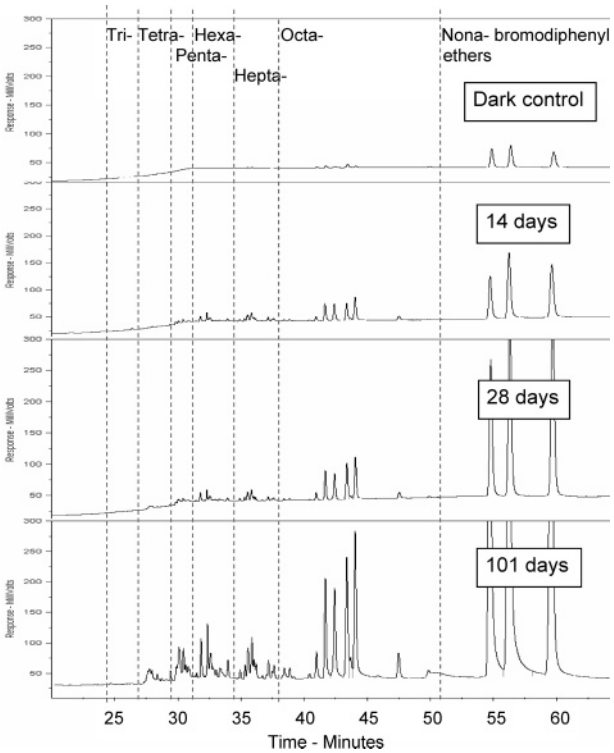

FIGURE 4. GC-ECD chromatograms showing appearance of PBDE congeners after sunlight irradiation of BDE-209 (retention time = 88.7 min) on montmorillonite at different times.

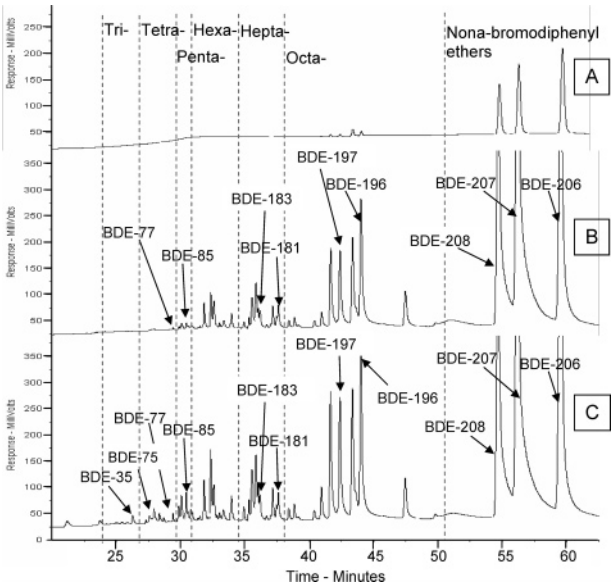

FIGURE 5. GC-ECD chromatograms of concentrated dark control (A) and sunlight-irradiated kaolinite (B) and montmorillonite (C) samples at 56 days: The retention time of BDE-209 is 88.7 min (off-scale), and the nonabromodiphenyl ethers within the dark control are present in the stock material.

drite, aluminum hydroxide, and birnessite in this study. Therefore, indirect photolysis, or reactions with the photogenerated active oxygen species, is not likely to play a significant role in the BDE-209 photodegradation on these minerals.

BDE-209 Debromination and Products. During BDE-209 photolysis, less brominated congeners were formed, and product retention times were compared to those of known congeners in an analytical reference standard. Table 1 contains GC-ECD relative retention times and other information for the PBDE standards. Only kaolinite and montmorillonite produced BDE-209 products with large enough concentrations to be detected by GC-ECD (Figures 2−4). Both lamp- and sunlight-irradiated samples showed similar product distributions and trends with time of irradiation. Over time, the areas of the peaks for nona-, octa- and heptabromodiphenyl ethers increased, with less brominated congener peaks appearing after 3 days in lamp-irradiated samples and after 14 days in sunlight-irradiated samples (Figures 3 and 4). Those peaks on the dark control sample chromatogram shown in Figures 4 and 5 are present in the stock material (i.e., appear at time zero) and are about 3% of the total PBDE peak area. Figure 4 shows less brominated congeners appearing via sequential debromination in the presence of montmorillonite with their peak areas increasing over time due to sunlight irradiation. A comparable but slower time trend was observed for kaolinite samples (data not shown), where the compounds' product distribution was similar between montmorillonite and kaolinite experiments (Figure 5).

These results indicate that the first step of degradation of BDE-209 is the loss of one bromine atom to form all three nonabromodiphenyl ether congeners followed by the subsequent formation of octabromodiphenyl ethers. Over time, the extent of debromination became significant as indicated by the increasing concentration and number of pentabromo- to tribromodiphenyl ether congeners appearing on chromatograms in kaolinite and montmorillonite samples (Figures 3−5). BDE-47 and -99, which are the dominant PBDE congeners detected in biota and humans, were not detected in this study; however, their precursors, BDE-196, -197, and -183 (*9*), were found on both clay minerals (Figure 5). In total, 28 and 34 products appeared on kaolinite and montmorillonite sample chromatograms, respectively (Figure 5). From the similar pattern of the appearance of product peaks between the two minerals, we conclude that the photodegradation rate is slightly slower on kaolinite than montmorillonite, thus accounting for the fewer product peaks observed. Significant differences in debromination patterns are not observed.

Previously reported debrominated products and patterns produced by photolysis of BDE-209 are similar to those found in this study. For example, BDE-209 has been shown to degrade to nona- to tetrabromodiphenyl ethers in various organic solvents by photolysis (*9*, *10*). Therefore, we can conclude that the type of sorbent will have had little to no effect on the debromination product distribution, although they do affect the rate of photodegradation. As a result, the clay mineral content of soils or sediments might be the key factor in controlling the rate of BDE-209 degradation by photolysis, but not its products.

Due to its extreme hydrophobicity, BDE-209 will occur in the environment predominately sorbed to solid phases and potentially may be transported to remote regions via particle attachment and transport. For example, the mass loading of mineral to the atmosphere is estimated to be 5000 Mt yr^{-1} on a global scale (*37*); these minerals include various clay minerals, such as smectite, kaolinite, and illite, as well as other noncrystalline materials (*23*). Also, it is well-known that annual dust storms travel thousands of miles from northeastern China over the Pacific Ocean and can be detected in the U.S. (*38*). If BDE-209 is attached to these particles, photodegradation to less brominated products is likely to occur, with transport of products occurring on a global scale. Indeed, air samples collected from Europe (*39*), Asia (*40*), and North America (*41*) have been shown to contain PBDEs. Air samples near the Great Lakes in the U.S. contained BDE-47, -99, -100, -153, and -154 (*41*), and their precursors, BDE-196, -197, and −183, were found in our experiments (Figure 5). The importance of PBDE photodegradation on

mineral aerosols and other types of aerosols, as well as particle−air phase distribution within the atmosphere, needs to be assessed further.

Acknowledgments

The research was financially supported by the Environmental Protection Agency, Office of Exploratory Research, Grants R-83025101-0 and R-83039801-0.

Literature Cited

(1) Bromine Science and Environmental Forum. *Total market demand*. http://www.bsef.com/ (accessed April 8, 2005).
(2) Hites, R. A. Polybrominated diphenyl ethers in the environment and in people: A meta-analysis of concentrations. *Environ. Sci. Technol.* **2004**, *38*, 945−956.
(3) de Wit, C. A. An overview of brominated flame retardants in the environment. *Chemospher.* **2002**, *46*, 583−624.
(4) Schecter, A.; Päpke, O.; Tung, K.-C.; Staskal, D.; Birnbaum, L. Polybrominated diphenyl ethers contamination of United States food. *Environ. Sci. Technol.* **2004**, *38*, 5306−5311.
(5) Luross, J. M.; Alaee, M.; Sergeant, D. B.; Whittle, D. M.; Solomon, K. R. Spatial and temporal distribution of polybrominated diphenyl ethers in lake trout from the great lakes. *Organohalogen Compd.* **2000**, *47*, 73−76.
(6) Meerts, I. A. T. M.; van Zanden, J. J.; Luijks, E. A. C.; van Leewen-Bol, I.; Marsh, G.; Jakobsson, E.; Bergman, Å.; Brouwer, A. Potent competitive interactions of some brominated flame retardants and related compounds with human transthyretin in vitro. *Toxicol. Sci.* **2000**, *56*, 95−104.
(7) Darnerud, P. O.; Eriksen, G. S.; Jóhannesson, T.; Larsen, P. B.; Viluksela, M. Polybrominated diphenyl ethers: Occurrence, dietary exposure, and toxicology. *Environ. Health Perspect.* **2001**, *109*, 49−68.
(8) Gerecke, A. C.; Hartmann, P. C.; Heeb, N. V.; Kohler; H.-P. E.; Giger W.; Schimid, P.; Zennegg, M.; Kohler, M. Anaerobic degradation of decabromodiphenyl ether. *Environ. Sci. Technol.* **2005**, *39*, 1078−1083.
(9) Bezares-Cruz, J.; Chad, T. J.; Hua, I. Solar photodecomposition of decabromodiphenyl ether: Products and quantum yield. *Environ. Sci. Technol.* **2004**, *38*, 4149−4156.
(10) Eriksson, J.; Green, N.; Marsh, G.; Bergman, Å. Photochemical decomposition of 15 polybrominated diphenyl ether congeners in methanol/water. *Environ. Sci. Technol.* **2004**, *38*, 3119−3125.
(11) Braekevelt, E.; Tittlemier, S. A.; Tomy, G. T. Direct measurement of octanol−water partition coefficients of some environmentally relevant brominated diphenyl ether congeners. *Chemosphere.* **2003**, *51*, 563−567.
(12) Söderström, G.; Sellström, U.; de Wit, A. C.; Tysklind, M. Photolytic debromination of decabromodiphenyl ether (BDE 209). *Environ. Sci. Technol.* **2004**, *38*, 127−132.
(13) Hua, I.; Kang, N.; Chad, T. J.; Fábrega-Duque, J. Heterogeneous photochemical reactions of decabromodiphenyl ether. *Environ. Toxicol. Chem.* **2003**, *22*, 798−804.
(14) Katagi, T. Photodegradation of esfenvalerate in clay suspensions. *J. Agric. Food Chem.* **1993**, *41*, 2178−2183.
(15) Miller, G. C.; Zepp, R. G. Effects of suspended sediments on photolysis rates of dissolved pollutants, *Water Res.* **1978**, *13*, 453−459.
(16) Mathew, R.; Khan, S. U. Photodegradation of metolachlor in water in the presence of soil mineral and organic constituents. *J. Agric. Food Chem.* **1996**, *44*, 3996−4000.
(17) Katagi, T. Photodegradation of the pyrethroid insecticide Esfenvalerate on soil, clay minerals, and humic acid surfaces. *J. Agric. Food Chem.* **1991**, *39*, 1351−1356.
(18) Karickhoff, S. W.; Bailey, G. W. Optical absorption spectra of clay minerals, *Clays Clay Miner.* **1973**, *21*, 59−70.
(19) Ciani, A.; Goss, K.-U.; Schwarzenbach, R. P. Light penetration in soil and particulate minerals. *Eur. J. Soil Sci.* **2005**, in press (doi: 10.1111/j.1365-2389.2005.00688.x).
(20) Kakegawa, N.; Kondo, T.; Ogawa, M. Variation of electron-donating ability of smectites as probed by photoreduction of methyl viologen. *Langmuir.* **2003**, *19*, 3578−3583.
(21) Ikonomou, M. G.; Rayne, S.; Addison, R. F. Exponential Increases of the Brominated Flame Retardants, Polybrominated Diphenyl Ethers, in the Canadian arctic from 1981 to 2000. *Environ. Sci. Technol.* **2002**, *36*, 1886−1892.
(22) Arnold, E.; Merrill, J.; Leinen, M.; King, J. The effect of source area and atmospheric transport on mineral aerosol collected over the North Pacific Ocean. *Global Planet Change* **1998**, *18*, 137−159.
(23) Shi, Z.; Shao, L.; Jones, T. P.; Lu, S. Microscopy and mineralogy of airborne particles collected during severe dust storm episodes in Beijing, China. *J. Geophysic. Res.* **2005**, *110*, D01303.
(24) Dixon, J. B.; Weed, S. B., In *Minerals in Soil Environments*; Soil Science Society of America: Madison, WI, 1989.
(25) Santamarina, J. C.; Klein, K. A.; Wang, Y. H.; Prencke, E. Specific surface: Determination and relevance. *Can. Geotech. J.* **2002**, *39*, 233−241.
(26) Schwertmann, U.; Cornell, R. M. In *Iron oxides in the laboratory*; VCH Verlagsgesellschaft: Weinheim, Germany, 1991.
(27) McKenzie, R. M. The synthesis of birnessite, cryptomelane, and some other oxides and hydroxides of manganese. *Mineral. Mag.* **1971**, *38*, 493−502.
(28) Huang, P. M.; Wang, T. S. C.; Wang, M. K.; Wu, M. H.; Hsu, N. W. Retention of phenolic acids by noncrystalline hydroxy-aluminum and iron compounds and clay minerals of soils. *Soil Sci.* **1977**, *123*, 213−219.
(29) Sellström, U.; Söderström, G.; de Wit, C.; Tysklind, M. Photolytic debromination of decabromodiphenyl ether (DeBDE). *Organohalogen Compd.* **1998**, *35*, 447−450.
(30) Shirozu, H. In *Introduction to clay mineralogy*. Fundamentals for clay science; Shirozu, H., Ed.; Asakura Publication: Tokyo, 1988.
(31) Konstantinou, I. K.; Zarkadis, A. K.; Albanis, T. A. Photodegradation of selected herbicides in various natural waters and soils under environmental conditions. *J. Environ. Qual.* **2001**, *30*, 121−130.
(32) Canonica, S.; Jans, U.; Stemmler, K.; Hoigne, J. Transformation kinetics of phenols in water: Photosensitization by dissolved natural organic material and aromatic ketones. *Environ. Sci. Technol.* **1995**, *29*, 1822−1831.
(33) Miller, G. C.; Zepp, R. C. Effect of suspended sediments on photolysis rates of dissolved pollutants. *Water Res.* **1979**, *13*, 453−459.
(34) Bachman, J.; Patterson, H. Photodecomposition of the carbamate pesticide carbofuran: kinetics and the influence of dissolved organic matter. *Environ. Sci. Tehcnol.* **1999**, *33*, 874−881.
(35) Fujihira, M.; Satoh, Y.; Osa, T. Heterogeneous photocatalystic oxidation of aromatic compounds on TiO_2. *Nature* **1981**, *293*, 206−208.
(36) Faust, B. C.; Hoigné, J., Photolysis of Fe(III)-hydroxy complexes as sources of OH radicals in clouds, fog, and rain. *Atmos. Environ.* **1990**, *23*, 235−240.
(37) Andreae, M. O. Climatic effects of changing atmospheric aerosol levels, In *World Survey of Climatology*, *Future Climates of the World*; Henderson-Sellers, A., Ed.; Elsevier: Amsterdam, 1995; Vol. 16, pp 341−392.
(38) Uno, I.; Amano, H.; Emori, S.; Kinoshita, K.; Matsui, I.; Sugimoto, N. Trans-Pacific yellow sand transport observed in April 1998: A numerical simulation. *J. Geophys. Res.* **2001**, *106*, 18331−18344.
(39) Bergander, L.; Kierkegaard, A.; Sellström, U.; Wideqvist, U.; de Wit, C. In *6th Nordic Symposium on Organic Pollutants*; Are brominated flame retardants present in ambient air? Smygehuk, September, 1995.
(40) Watanabe, I.; Kawano, M.; Tatsukawa, R. Polybrominated and mixed polybromo/chlorinated dibenzo-*p*-dibenzofurans in the Japanese environment. *Organohalogen Compd.* **1995**, *24*, 337−340.
(41) Dodder, N. G.; Strandberg, B.; Hites, R. A. Concentrations and spatial variations of polybrominated diphenyl ethers in fish and air from the northeastern United States. *Organohalogen Compd.* **2000**, *47*, 69−72.

Received for review July 20, 2005. Revised manuscript received October 24, 2005. Accepted October 25, 2005.

ES051415T